

## **Biomass gasification in microwave plasma**

### **An experimental feasibility study with a side stream from a fermentation reactor**

Delikonstantis, Evangelos; Sturm, Guido; Stankiewicz, Andrzej I.; Bosmans, Anouk; Scapinello, Marco; Dreiser, Christian; Lade, Oliver; Brand, Stefan; Stefanidis, Georgios D.

**DOI**

[10.1016/j.cep.2019.107538](https://doi.org/10.1016/j.cep.2019.107538)

**Publication date**

2019

**Document Version**

Accepted author manuscript

**Published in**

Chemical Engineering and Processing - Process Intensification

**Citation (APA)**

Delikonstantis, E., Sturm, G., Stankiewicz, A. I., Bosmans, A., Scapinello, M., Dreiser, C., Lade, O., Brand, S., & Stefanidis, G. D. (2019). Biomass gasification in microwave plasma: An experimental feasibility study with a side stream from a fermentation reactor. *Chemical Engineering and Processing - Process Intensification*, 141, Article 107538. <https://doi.org/10.1016/j.cep.2019.107538>

**Important note**

To cite this publication, please use the final published version (if applicable).  
Please check the document version above.

**Copyright**

Other than for strictly personal use, it is not permitted to download, forward or distribute the text or part of it, without the consent of the author(s) and/or copyright holder(s), unless the work is under an open content license such as Creative Commons.

**Takedown policy**

Please contact us and provide details if you believe this document breaches copyrights.  
We will remove access to the work immediately and investigate your claim.

# Biomass gasification in microwave plasma: an experimental feasibility study with a side stream from a fermentation reactor

*Evangelos Delikonstantis<sup>a</sup>, Guido Sturm<sup>b</sup>, Andrzej I. Stankiewicz<sup>b</sup>, Anouk Bosmans<sup>a</sup>, Marco Scapinello<sup>a</sup>, Christian Dreiser<sup>c</sup>, Oliver Lade<sup>c</sup>, Stefan Brand<sup>c</sup> and Georgios D. Stefanidis<sup>a,b\*</sup>*

<sup>a</sup> Process Engineering for Sustainable Systems (ProcESS), Department of Chemical Engineering KU Leuven, Celestijnenlaan 200F, 3001 Leuven, Belgium

<sup>b</sup> Intensified Reaction & Separation Systems, Process & Energy Department, Delft University of Technology, Leeghwaterstraat 39, 2628 CB Delft, The Netherlands

<sup>c</sup> Clariant, Group Process Technology, Brueningstrasse 50, 65926 Frankfurt am Main, Germany

## Corresponding Author

\*Georgios D. Stefanidis

Tel: +32(0)16321007

e-mail: georgios.stefanidis@kuleuven.be

## ABSTRACT

In this work, we report on air/N<sub>2</sub> gasification of a byproduct stream from an industrial fermenter in a tubular microwave plasma reactor to investigate the feasibility of the technology for organic compounds valorization, given the limited number of relevant works in the literature. In this context, an operating window defined by air/N<sub>2</sub>/biomass flow rates and power input has been identified to enable stable and efficient operation. Up to 89% carbon conversion efficiency and 41% cold gas efficiency have been attained with syngas product composition H<sub>2</sub>:CO:CO<sub>2</sub> = 41:53:6, fairly close to the calculated equilibrium composition values in the temperature range 973 K to 2173 K.

**Keywords:** microwave plasma, gasification, biomass, syngas, circular economy

## 1. Introduction

There is a pressing need for development of efficient and scalable process routes for transformation of renewable biomass to fuels and chemicals due to the rapid fossil feedstock depletion and greenhouse gas emissions increase [1]. In this context, different widely available and inexpensive biomass feedstocks, such as agricultural residues, food waste, sawdust and wood have been investigated [2]. Among the different thermochemical processes for biomass upgrading, pyrolysis and gasification are the most mature ones. In particular, gasification, that is biomass thermal cracking in presence of an oxidizing agent (air, O<sub>2</sub>, steam [20] or CO<sub>2</sub> [8]) promotes formation of syngas [3,4], which can be utilized either for heat and electricity generation [5] or for fuels and chemicals through e.g. the Fischer-Tropsch process [6]. Although conventional biomass gasification has been launched at commercial scale [7], the process still faces limitations, such as elevated operating pressures, incomplete gasification resulting in volatile sludge, slugs and tar, pretreatment of the feed (drying and shredding) with impact on the production cost [8], and long heat-up periods during startup.

Plasma gasification can address some of the above challenges. The high temperature of plasma, the generation of active species and the radiation intensity can initiate reactions that are hardly activated in conventional gasification, thus, heavy species are fully cracked, impurities melt and inorganic fraction is vitrified into a non-leachable slag [8]. Consequently, higher purity syngas is produced. In addition, the higher energy densities attained in the plasma zone increase the reagents mixture activity, decreasing the amount of oxidizing agent needed. Therefore, lower gas stream volumes are produced and lower reactor volumes are needed [9]. Finally, plasma driven gasifiers feature short start-up and shut-down periods and high energy densities [10], opening up possibilities for the utilization of fluctuating renewable energy sources, e.g. solar and wind energy.

Among different plasma technologies, arc plasma torch has extensively been used for organic material gasification [11]. However, the limited high voltage electrode lifespan due to moisture [12] or other corrosive substances contained in the feedstock, product contamination with the electrode fabrication

material caused by electrode erosion [13] and the high parasitic load, which leads to low energy efficiency (the power output can be as low as 50% of the power input [14]), are disadvantages of the technology. Microwave (MW) plasma has been efficiently used for gaseous and liquid (oxygenated) hydrocarbon conversion [15-17] and recently emerged as an alternative electrodeless plasma technology for biomass treatment. The absence of electrodes has some advantages compared to AC, DC plasma torches, such as higher process stability (plasma is not affected by contamination or erosion), longer operating periods and less maintenance. On the other side, design of microwave plasma reactors for gasification of solid organic material is rather complicated and challenging, therefore only few relevant works have been published in the literature. To our knowledge, these include brown coal [18], algae [19], wood chips [20] and cellulose [21], prior art of our group.

Herein, MW plasma-assisted gasification of a multicomponent byproduct stream from a fermentation reactor including sugar, lignin, water solubles, acids, proteins and ashes (predominantly silica), henceforth referred to as ‘raw lignin’, with an average ash-free elemental composition of  $\text{CH}_{1.50}\text{O}_{0.49}$ , is investigated. Such a complex substance mixture is not suitable for chemical processing due to the need for complex separation steps and tailored catalysts and solvents for valorization of the different mixture components into added value products. A mixture of air and  $\text{N}_2$  is used as oxidizing agent. A short parametric study is carried out to establish an operating window for stable operation and satisfactory technology performance in terms of syngas composition, carbon conversion efficiency (CCE, Eq. 1) and cold gas efficiency (CGE, Eq. 2). Syngas composition ( $\text{H}_2$ ,  $\text{CO}$  and  $\text{CO}_2$ ) from experiments is benchmarked against the composition predictions of a thermodynamic equilibrium model in the temperature range 973 K to 2173 K. This range was selected based on temperature measurements in microwave plasma experiments feeding only air/ $\text{N}_2$  mixtures at different flow rates without performing gasification. In these experiments, the minimum temperatures recorded at the outlet of the quartz pipe and 10 cm above the outlet were 890°C and 1080°C, respectively.

## 2. Materials and methods

### 2.1 MW plasma gasifier

A schematic representation of the plasma reactor assembly used in the gasification experiments is presented in Figure 1. The plasma reactor comprises an upper and a lower part. The upper part, where the plasma torch is ignited, is a vertically-oriented quartz pipe (31 mm ID, 33 mm OD) placed in the center of a larger waveguide and connected with the lower part through a metal tube. The lower part comprises a tube internally clad with quartz (50 mm long, 30 mm ID, 34 mm OD,  $c_p = 730 \text{ J/kg}\cdot\text{K}$ ;  $k = 1.40 \text{ W/m}\cdot\text{K}$  and  $T_{\text{melt}} = 1986 \text{ K}$ ) and externally coated with an air-brass layer (to enhance heat transfer), encapsulated in a nickel-plated steel pipe support. Copper-based cooling coils placed around the nickel-plated steel pipe maintain the wall temperature at  $\sim 550 \text{ }^\circ\text{C}$  to prevent reactor thermal failure and tar condensation; water was utilized as cooling medium. Finally, a collection vessel cooled by water, which the reactor lower part ends into, is used for solids and ash removal.

Biomass solids ( $< 1 \text{ mm}$  particle size;  $D_{10} = 0.07 \text{ mm}$ ,  $D_{50} = 0.4 \text{ mm}$ ,  $D_{90} = 0.85 \text{ mm}$  obtained by sieve analysis) were fed into the reactor from the top and entrained by the direct flow of the feed gas which comprised a carrier gas ( $\text{N}_2$ ) and the gasifying agent (air). The feed gas was initially mixed with biomass solids in a steel vessel. An auxiliary gaseous stream (swirl gas) of the same composition as the feed gas was concurrently blown via a set of nozzles, enabling vortex flow conditions that confined the torch in the core zone of the reactor away from the reactor wall. Mass flow controllers (Bronkhorst F-201AV-50K) were employed to set the  $\text{N}_2$  and air flow rates. The plasma was powered by a MW field, which was generated by a 2.45-GHz magnetron of 6 kW maximum output power and propagated through a rectangular waveguide (WR-340). Other integral parts of the MW circuit were an isolator to prevent exposure of the magnetron to the reflected MW field, an impedance transformer to minimize reflections toward the magnetron and a tunable reflector to adjust the position of the MW field in the circuit. Direct contact of biomass with the plasma enabled biomass conversion to syngas. Ash was collected at the reactor bottom (collection vessel), whereas the gaseous product stream escaped from the vessel top and entered the

conditioning section prior to composition analysis. A sequence of heat exchangers was used to quench the syngas stream and remove tars by condensation (not quantified). Unreacted feedstock particles were recovered in a cyclone. The remaining moisture, fine solids and other contaminants were removed by filters employing activated carbon and calcium oxide prior to gas storage in sampling bags (Tedlar, 0.15 L). The composition of the purified syngas stream was analyzed by an offline micro-gas chromatograph (micro-GC, Varian CP-4900) equipped with CP-Molesieve 5 Å & PoraPlot U columns.

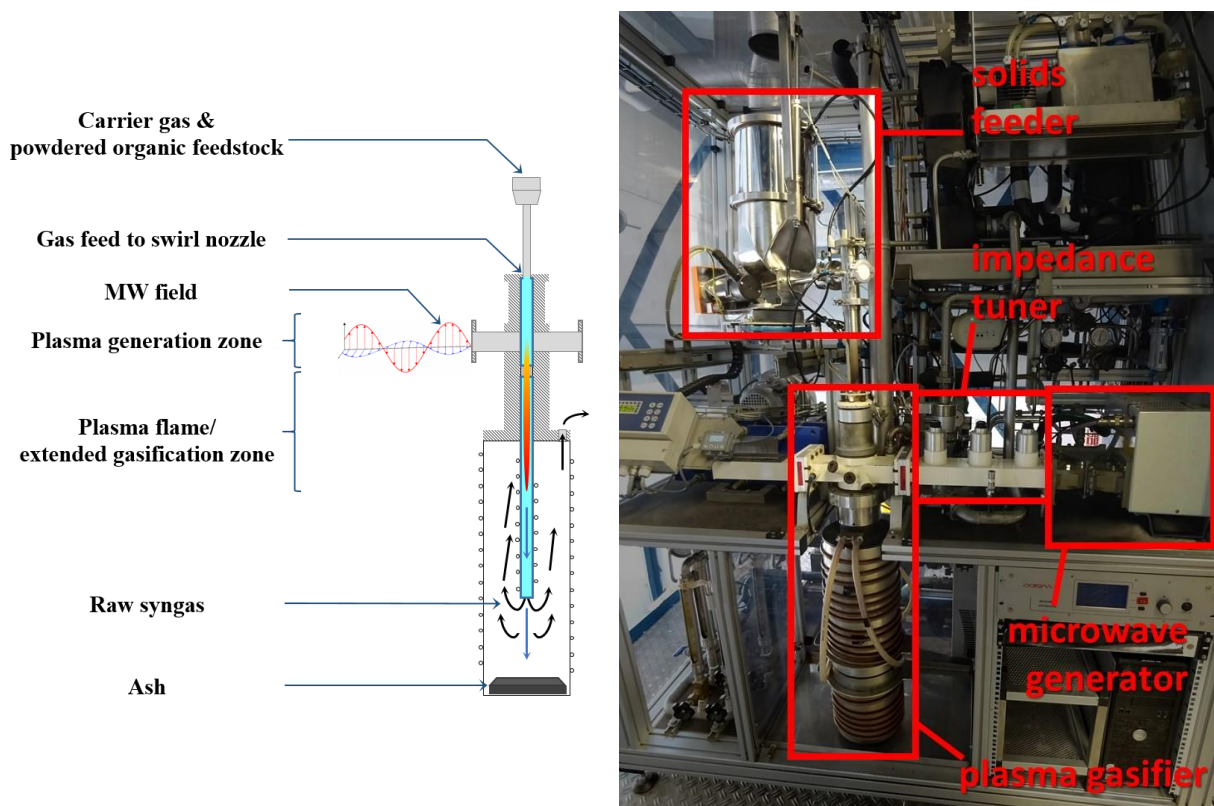


**Figure 1.** Experimental setup for microwave plasma assisted biomass gasification: Left) schematic of the microwave plasma reactor section; Right) photo of the entire experimental system highlighting (enclosed in the red frames) the microwave generator, the microwave plasma reactor, the impedance tuner and the biomass feeder.

## 2.2 Process performance criteria

Carbon conversion efficiency (CCE) and cold gas efficiency (CGE) were employed to assess the gasifier performance. Those quantities are defined by Equation 1 and 2, respectively:

$$CCE = \frac{\text{Total carbon out (product gas)}}{\text{Total carbon in (feed)}} \quad (1)$$

$$CGE = \frac{\dot{m}_{\text{syngas}} \cdot LHV_{\text{syngas}}}{\dot{m}_{\text{feed}} \cdot LHV_{\text{feed}} + P_{\text{torch}}} \quad (2)$$

where  $\dot{m}_{\text{syngas}}$  and  $LHV_{\text{syngas}}$  correspond to mass flow rate and lower heating value of the produced gas, respectively;  $\dot{m}_{\text{feed}}$ ,  $LHV_{\text{feed}}$  and  $P_{\text{torch}}$  correspond to mass flow rate, lower heating value of the fed biomass and magnetron power output, respectively.

The  $LHV_{\text{feed}}$  was theoretically calculated based on the higher heating value ( $HHV_{\text{feed}}$ ) on dry ash-free basis (daf) as in [22]. The  $HHV_{\text{daf}}$  was calculated using the correlations described in [23]. Considering the elemental analysis of the model compound used in this work (Table 1), the  $LHV_{\text{dry}}$  was calculated 19.6 MJ/kg, which is comparable to the calorific values of other biomass feedstocks reported in the literature [24].

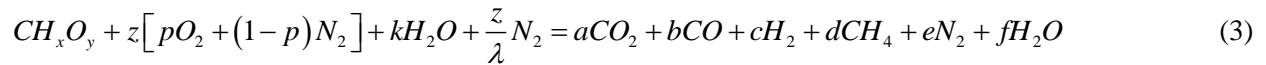
**Table 1.** Elemental analysis of the “raw lignin” ( $\text{CH}_{1.5}\text{O}_{0.49}$ ) used as feed for the gasification experiments expressed in as received (ar), dry and dry ash-free (daf) basis.

| Element  | Content              |                       |                       |
|----------|----------------------|-----------------------|-----------------------|
|          | wt <sub>ar</sub> [%] | wt <sub>dry</sub> [%] | wt <sub>daf</sub> [%] |
| Carbon   | 46.1                 | 47.5                  | 55.2                  |
| Hydrogen | 5.8                  | 6.0                   | 7.0                   |

|          |      |      |      |
|----------|------|------|------|
| Nitrogen | 1.2  | 1.2  | 1.4  |
| Oxygen   | 30.4 | 31.3 | 36.4 |
| Sulfur   | 0.1  | 0.1  | 0.1  |
| Ash      | 13.5 | 13.9 | -    |
| Moisture | 3.0  | -    | -    |

### 2.3 Thermodynamic equilibrium model

A thermodynamic equilibrium model was developed to benchmark the gasifier performance. The outlet stream composition was calculated by minimizing the Gibbs free energy of the reaction system. A non-stoichiometric and homogeneous formulation was adopted since neither the particular reaction mechanism was known, nor solid species were present in the outlet stream. The following gaseous species were considered to be present in the gasifier outlet stream: CO, CO<sub>2</sub>, H<sub>2</sub>, H<sub>2</sub>O, CH<sub>4</sub> and N<sub>2</sub>. Collectively, the global gasification reaction used in the thermodynamic model is described by Equation 3:



Cl and S that may be present in the feed were considered as traces; therefore, they were excluded from the equilibrium model [25]. N<sub>2</sub> contained in the air (gasifying agent) and also used as swirl flow was assumed non-reactive, although small amounts of NH<sub>3</sub>, HCN and nitrogenated tars may be formed in low amounts [26].

Regarding the global gasification reaction coefficients, k was defined by the feed moisture content (Table I); z was calculated from the equivalence ratio (experimental O<sub>2</sub>/feed ratio over the stoichiometric O<sub>2</sub>/feed ratio required for combustion); p was defined by the type of gasification agent (p = 0.21 for air) and λ is the experimental air/N<sub>2</sub> ratio (Table 2). The remaining coefficients in Equation 3 were calculated by the

elemental atomic balances of C, H, O and N (Equations 4, 5, 6 and 7, respectively) and the equilibrium constants for the water-gas shift (WGS) and steam methane reforming reaction (SMR) by Equations 8 and 9, respectively:

$$C: 1 = a + b + d \quad (4)$$

$$H: x + 2k = 2c + 4d + 2f \quad (5)$$

$$O: y + 2pz + k = 2a + b + f \quad (6)$$

$$N: z(1 - p) + \frac{z}{\lambda} = e \quad (7)$$

$$K_{WGS} = \frac{y_{H_2} \cdot y_{CO_2}}{y_{H_2O} \cdot y_{CO}} \quad (8)$$

$$K_{SMR} = \frac{y_{H_2}^3 \cdot y_{CO}}{y_{CH_4} \cdot y_{H_2O}} \quad (9)$$

where  $y_i$  is the molar fraction of the  $i$  species in the gasifier outlet stream;  $K_{WGS}$  and  $K_{SMR}$  are the equilibrium constants.

The equilibrium model was further simplified on the ground that models using air as gasifying agent predict lower  $CH_4$  concentration as compared to the other gases at atmospheric pressure and high temperatures [27]; thus,  $CH_4$  concentration was neglected and so  $d = 0$ . Finally,  $K_{WGS}$  and  $K_{SMR}$  values were calculated for the 973 K to 2173 K range, which is expected to cover the temperature range in the gasification zone of the reactor.

### 3. Results and discussion

#### 3.1 Biomass gasification experiments

In this section, the biomass gasification experiments performed in the microwave plasma reactor are reported and the reactor performance in terms of syngas product composition (gasifier outlet stream), carbon conversion efficiency (CCE) and cold gas efficiency (CGE) is presented and discussed. The biomass gasification experiments are structured in the context of a short parametric study, in which the impact of flow conditions variation namely, swirl gas flow and direct (feed) flow on plasma reactor performance is studied. Next, the syngas composition attained in the gasification experiments is compared to the predictions of the equilibrium model described in section 2.3.

Table 2 presents the different flow conditions applied during the MW plasma gasification experiments with raw lignin. Particularly, the swirl gas flow and direct (feed) flow rates are varied while the O<sub>2</sub>/biomass feed ratio is kept constant (= 0.3 on molar basis). Figure 2-left and Figure 2-right show syngas composition and CCE and CGE, respectively, for the five different sets of conditions applied.

**Table 2.** MW plasma gasification of raw lignin with an air/N<sub>2</sub> mixture at different tested swirl gas flows and direct (feed) flow rates. The biomass feed rate varies such that O<sub>2</sub>/biomass feed ratio = 0.3 on molar basis in all experiments. The net microwave power dissipated in the plasma reactor (forward – reflected power) varies depending on the chosen process parameters.

| Case | Description              | Direct flow | Swirl flow | Air/N <sub>2</sub> | Biomass feed | Net power |
|------|--------------------------|-------------|------------|--------------------|--------------|-----------|
| No   |                          | NI/min      | NI/min     | NI/min             | g/s          | kW        |
| 1    | Base case                | 5           | 30         | 10/25              | 0.13         | 2.4       |
| 2    | Constant swirl gas flow  | 5           | 25         | 8.5/21.5           | 0.11         | 2.3       |
| 3    |                          | 5           | 20         | 7.1/17.9           | 0.09         | 2.3       |
| 4    | Constant total (direct   | 7.5         | 27.5       | 10/25              | 0.13         | 2.1       |
| 5    | +swirl) flow (35 NI/min) | 10          | 25         | 10/25              | 0.13         | 2.4       |

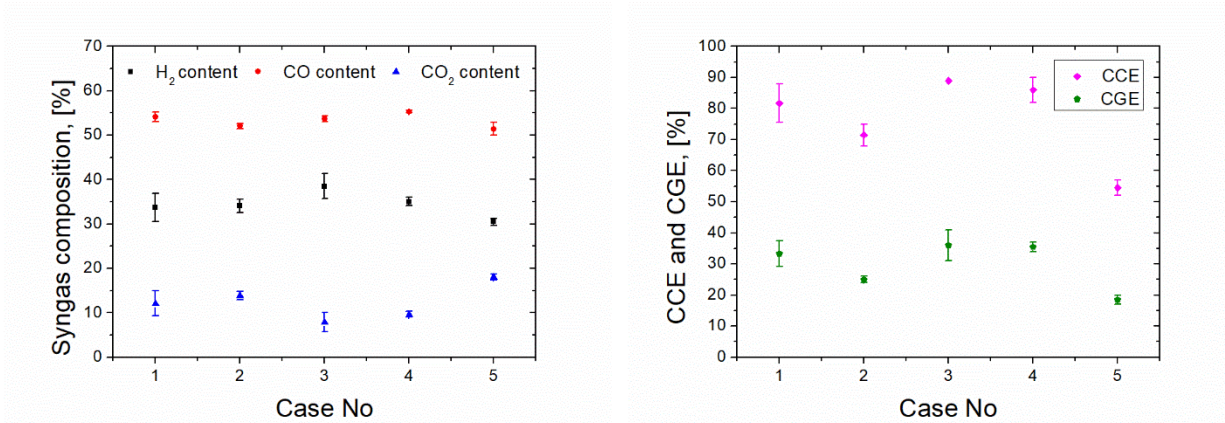


**Figure 2.** *left:* syngas product composition (H<sub>2</sub>, CO, CO<sub>2</sub> % molar content) from the MW plasma gasifier under different tested flow conditions; *right:* carbon conversion efficiency (CCE) and cold gas efficiency (CGE) of the MW plasma gasifier under different tested flow conditions (Cases 1 to 5 as reported in Table 2). Composition data were collected after 170 s from the start of experiment when steady state was reached.

In the narrow operating window examined, syngas composition appears to be relatively stable as shown in Figure 2-left. Only in Case 5, somewhat lower amounts of H<sub>2</sub> and CO are produced as compared to the other cases, probably due to the higher direct flow rate and consequently lower biomass residence time in the reactor. CCE and CGE for the five cases are shown in Figure 2-right, following the same trend as in Figure 2-left, namely relatively stable values with the exception of Case 5 (maximum direct flow rate/minimum residence time), where CCE and CGE are decreased due to the decreased syngas composition shown in Figure 2-left and the somewhat higher net power consumption reported in Table 2. The maximum CCE and CGE values obtained were 89% and 41%, respectively, in Case 3. In the literature, cold gas efficiencies up to ~81% have been reported for large-scale gasifiers that mainly process relatively well-defined feedstocks (biomass, coal) and operate at above-atmospheric pressures using either pure O<sub>2</sub>, or steam/O<sub>2</sub>, or air/O<sub>2</sub> mixtures as oxidants [28]. The aim of the current work is to investigate the feasibility of the relatively new microwave plasma gasification technology at laboratory scale using a real industrial

fermenter by-product. Further work is needed on scale up of the process as well as optimization of the gas-solid flow patterns and insulation of the reactor to increase CGE.

### 3.2 Comparison with equilibrium predictions

To assess reactor performance, outlet H<sub>2</sub>, CO and CO<sub>2</sub> fractional yields (% mol) are compared in Figure 3 with the predictions of the thermodynamic equilibrium model described in section 2.3 (Eq. Model) over the temperature range 973 K to 2173 K. The average H<sub>2</sub>, CO and CO<sub>2</sub> fractional yields considering all experiments performed (Exp. Avrg) and the fractional yields of H<sub>2</sub>, CO and CO<sub>2</sub> obtained in Case 3 (Exp. Max; maximum CCE and CGE case) are also depicted in Figure 3, while the colored areas depict the upper and lower confidence bounds of the average experimental points. Since the gasification temperature was not measured over the course of the biomass gasification experiments, the experimental results are presented as straight horizontal lines (average fractional yields) and square symbols (fractional yields in Case 3) along the reaction temperature axis.

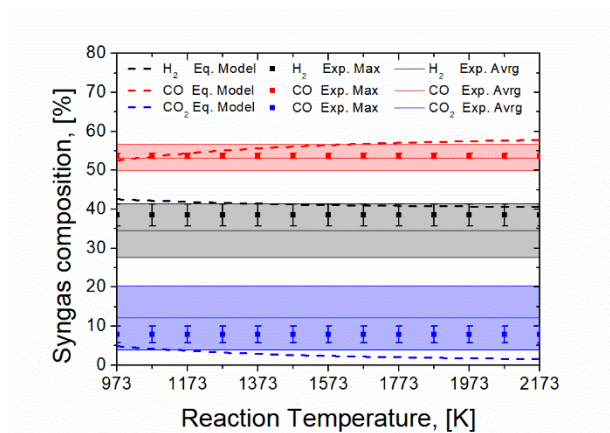


**Figure 3.** Comparison between experimental syngas composition [average H<sub>2</sub>, CO and CO<sub>2</sub> fractional yields over the five cases in Table 2 (Exp. Avrg) and H<sub>2</sub>, CO and CO<sub>2</sub> fractional yields in the case of maximum CCE and CGE (Exp. Max, Case 3)] and equilibrium predictions over the temperature range 973 K to 2173 K. The colored areas depict the upper and lower confidence bounds of the average experimental points.

Figure 3 shows that the average CO fractional yield is very close to the equilibrium predictions. In Case 3, the maximum deviation from equilibrium is 7.2% for the examined temperature range. As regards to H<sub>2</sub>, the maximum deviation between Case 3 and equilibrium model is 9.6%. In the case of CO<sub>2</sub>, both the average yield fraction and the yield fraction corresponding to Case 3 exceed the equilibrium predictions. This trend was also presented in [26] and [29] and was attributed to the assumptions made to simplify the equilibrium model that is also used in this work.

#### **4. Conclusions**

Information on the application of microwave plasma technology to biomass valorization is scarce in the literature. In this work, microwave plasma gasification experiments in continuous flow using a real fermenter by-product stream and an air/N<sub>2</sub> mixture were carried out at different flow conditions to assess the suitability of the microwave plasma technology in this field. An operating window, defined by air/N<sub>2</sub>/biomass flow rates and power input, was established in which high carbon conversion efficiency (89%) and near equilibrium syngas composition (H<sub>2</sub>:CO:CO<sub>2</sub> = 41:53:6) was obtained. The maximum cold gas efficiency of 41% reported can be substantially improved with a) proper insulation of the reactor to minimize energy losses and b) optimization of the flow patterns (swirl and direct feed flow) to maximize the contact of the hot plasma zone and the biomass particles, thus making the use of microwave power applied more efficient.

#### **Acknowledgements**

We would like to thank the Bill and Melinda Gates Foundation and CLARIANT for financial support to the development of the microwave plasma gasification setup. Mr. Javier Leyva Rico is thanked for carrying out the gasification experiments. Verborg Engineering B.V. is thankfully acknowledged for their active technical assistance.

## References

- [1] S.J. Gerssen-Gondelach, D. Saygin, B. Wicke, M.K. Patel, A.P.C. Faaij, Competing uses of biomass: Assessment and comparison of the performance of bio-based heat, power, fuels and materials, *Renew. Sustain. Energy Rev.* 40 (2014) 964–998. doi:10.1016/j.rser.2014.07.197.
- [2] L.A. Pfaltzgraff, M. De Bruyn, E.C. Cooper, V. Budarin, J.H. Clark, Food waste biomass: A resource for high-value chemicals, *Green Chem.* 15 (2013) 307–314. doi:10.1039/c2gc36978h.
- [3] H. Knoef, J. Ahrenfeldt, *Handbook biomass gasification*, BTG biomass technology group, The Netherlands, 2005.
- [4] C. Higman, M. v. d. Burgt, *Gasification*, second ed., UK, Elsevier, 2008.
- [5] J.A. Ruiz, M.C. Juárez, M.P. Morales, P. Muñoz, M.A. Mendívil, Biomass gasification for electricity generation: Review of current technology barriers, *Renew. Sustain. Energy Rev.* 18 (2013) 174–183. doi:10.1016/j.rser.2012.10.021.
- [6] S. Heidenreich, P.U. Foscolo, New concepts in biomass gasification, *Prog. Energy Combust. Sci.* 46 (2015) 72–95. doi:10.1016/j.peccs.2014.06.002.
- [7] Wabash River Coal Gasification Repowering Project, [http://physics.oregonstate.edu/~hetheriw/energy/topics/doc/elec/coal/igcc/Wabash\\_River\\_Coal\\_Gasification\\_Repowering\\_Project,\\_Clean\\_Coal\\_Technology\\_Compendium.htm](http://physics.oregonstate.edu/~hetheriw/energy/topics/doc/elec/coal/igcc/Wabash_River_Coal_Gasification_Repowering_Project,_Clean_Coal_Technology_Compendium.htm), 1999 (Accessed 1 October 2018).
- [8] A.L. Sanchez, (2010) European Patent Application No EP2163597A1. Munich, Germany: European Patent Office.
- [9] I. Janajreh, S.S. Raza, A.S. Valmundsson, Plasma gasification process: Modeling, simulation and comparison with conventional air gasification, *Energy Convers. Manag.* 65 (2013) 801–809.

doi:10.1016/j.enconman.2012.03.010.

- [10] E. Gomez, D.A. Rani, C.R. Cheeseman, D. Deegan, M. Wise, A.R. Boccaccini, Thermal plasma technology for the treatment of wastes: A critical review, *J. Hazard. Mater.* 161 (2009) 614–626. doi:10.1016/j.jhazmat.2008.04.017.
- [11] A. Sanlisoy, M.O. Carpinlioglu, A review on plasma gasification for solid waste disposal, *Int. J. Hydrogen Energy.* 42 (2017) 1361–1365. doi:10.1016/j.ijhydene.2016.06.008.
- [12] S.J. Yoon, J. Goo Lee, Syngas production from coal through microwave plasma gasification: Influence of oxygen, steam, and coal particle size, *Energy and Fuels.* 26 (2012) 524–529. doi:10.1021/ef2013584.
- [13] G. Bonizzoni, E. Vassallo, Plasma physics and technology; Industrial applications, *Vacuum.* 64 (2002) 327–336. doi:10.1016/S0042-207X(01)00341-4.
- [14] Energy Recovery Council, Pyrolysis gasification, process and technology. <http://energyrecoverycouncil.org/>, 2018 (Accessed 1 October 2018)
- [15] J. Mizeraczyk, K. Urashima, M. Jasinski, M. Dors, Hydrogen production from gaseous fuels by plasmas - A review, *Int. J. Plasma Environ. Sci. Technol.* 8 (2014) 89–97.
- [16] D. Czylkowski, B. Hrycak, M. Jasiński, M. Dors, J. Mizeraczyk, Microwave plasma-based method of hydrogen production via combined steam reforming of methane, *Energy.* 113 (2016) 653–661. doi:10.1016/j.energy.2016.07.088.
- [17] R. Miotk, B. Hrycak, D. Czylkowski, M. Dors, M. Jasinski, J. Mizeraczyk, Liquid fuel reforming using microwave plasma at atmospheric pressure, *Plasma Sources Sci. Technol.* 25 (2016). doi:10.1088/0963-0252/25/3/035022.
- [18] Y.C. Hong, S.J. Lee, D.H. Shin, Y.J. Kim, B.J. Lee, S.Y. Cho, H.S. Chang, Syngas production from

- gasification of brown coal in a microwave torch plasma, *Energy*. 47 (2012) 36–40. doi:10.1016/j.energy.2012.05.008.
- [19] K.C. Lin, Y.C. Lin, Y.H. Hsiao, Microwave plasma studies of *Spirulina* algae pyrolysis with relevance to hydrogen production, *Energy*. 64 (2014) 567–574. doi:10.1016/j.energy.2013.09.055.
- [20] C.J. Lupa, S.R. Wylie, A. Shaw, A. Al-Shamma'A, A. J. Sweetman, B.M.J. Herbert, Experimental analysis of biomass pyrolysis using microwave-induced plasma, *Fuel Process. Technol.* 97 (2012) 79–84. doi:10.1016/j.fuproc.2012.01.015.
- [21] G.S.J. Sturm, A.N. Munoz, P. V. Aravind, G.D. Stefanidis, Microwave-Driven Plasma Gasification for Biomass Waste Treatment at Miniature Scale, *IEEE Trans. Plasma Sci.* 44 (2016) 670–678. doi:10.1109/TPS.2016.2533363.
- [22] P. Quaak, H. Knoef, H. Stassen, *Energy from Biomass: A review of combustion and gasification technologies*, World Bank Tech. Pap. (1999) 1–78. doi:ISBN 0 -8213-4335-1.
- [23] S.A. Channiwala, P.P. Parikh, A unified correlation for estimating HHV of solid, liquid and gaseous fuels, *Fuel*. 81 (2002) 1051–1063. doi:10.1016/S0016-2361(01)00131-4.
- [24] B. Boundy, S.W. Diegel, L. Wright, S.C. Davis, *Biomass Energy Data Book*, fourth ed., 2011.
- [25] N. Jand, V. Brandani, P.U. Foscolo, Thermodynamic limits and actual product yields and compositions in biomass gasification processes, *Ind. Eng. Chem. Res.* 45 (2006) 834–843. doi:10.1021/ie050824v.
- [26] A. Gómez-Barea, B. Leckner, Modeling of biomass gasification in fluidized bed, *Prog. Energy Combust. Sci.* 36 (2010) 444–509. doi:10.1016/j.peccs.2009.12.002.
- [27] K.T. Wu, R.Y. Chein, Modeling of Biomass Gasification with Preheated Air at High Temperatures, *Energy Procedia*. 75 (2015) 214–219. doi:10.1016/j.egypro.2015.07.307.

- [28] E4tch, Review of Technologies for Gasification of Biomass and Wastes. <http://www.e4tech.com/wp-content/uploads/2016/01/gasification2009.pdf>, 2009 (Accessed 3 October 2018)
- [29] C.R. Altafini, P.R. Wander, R.M. Barreto, Prediction of the working parameters of a wood waste gasifier through an equilibrium model, *Energy Convers. Manag.* 44 (2003) 2763–2777. doi:10.1016/S0196-8904(03)00025-6.